*Journal of Sound and Vibration* (2001) **246**(5), 877–899
doi:10.1006/jsvi.2001.3675, available online at http://www.idealibrary.com on IDEAL®

# A UNIFIED METHOD FOR CONSTRUCTING THE DYNAMIC BOUNDARY STIFFNESS AND BOUNDARY FLEXIBILITY FOR ROD, BEAM AND CIRCULAR MEMBRANE STRUCTURES

J. T. Chen and I. L. Chung

*Department of Harbor and River Engineering, National Taiwan Ocean University, P.O. Box 7-59, Keelung, Taiwan, Republic of China. E-mail: jtchen@mail.ntou.edu.tw*

(*Received* 2 *August* 2000, *and in final form* 9 *March* 2001)

In this paper, the dynamic boundary stiffness and boundary flexibility for rod, beam and circular membrane structures are analytically derived using the dual integral formulation. Two approaches, the real- and the imaginary-part kernels are employed to determine the dynamic boundary stiffness and boundary flexibility. The continuous system for a circular membrane can be transformed into a discrete system with a circulant matrix. Based on the properties of circulant, the analytical solution for dynamic boundary stiffness and dynamic boundary flexibility in the discrete system can be derived. The exact formulae for the dynamic boundary stiffness and boundary flexibility matrices of a rod, a beam and a circular membrane are obtained. Also, the calculation for the static flexibility using the pseudo-inverse technique is discussed. 

## 1. INTRODUCTION

Stiffness and flexibility matrices play important roles in structural analysis [1]. This concept can be easily extended to dynamic stiffness and dynamic flexibility if harmonic loading is applied [2]. Many approaches can be considered to determine the stiffnesses and flexibility, e.g., analytical method, finite element method (FEM) and boundary element method (BEM). Various analytical solutions of dynamic stiffnesses can be found in the textbook of structural dynamics [2]. In FEM, Mario and Lam derived the closed-form solution for general stiffness matrix of a Bernouli–Euler beam and extended the solution to a series form [3, 4]. It is interesting to find that the procedure in deriving stiffness by Mario and Lam is contrary to the derivation using the multiple reciprocity method (MRM) developed by Chen's group [5, 6] as shown in Table 1. The effects of shear deformation and rotatory inertia were considered by Banerjee [7]. Later, the effect of axial force was addressed [8]. The dynamic stiffness for two- and three-dimensional cases can be found in references [9–11]. The dynamic stiffness can be determined by using indirect BEM [12] or direct method [13]. Both methods employed the complex-valued kernels. Although the dynamic stiffness matrices for simple structures (rod and beam) have been found by FEM [14], an alternative derivation using the dual formulation will be considered here. The dynamic stiffness derived by BEM focuses on the relationship between boundary force and boundary displacement. We can term it "dynamic boundary stiffness". The zeros and anti-zeros for the structure system are imbedded in the dynamic stiffness and dynamic flexibility. The zero of dynamic stiffness indicates the resonance frequency or critical wave number, while the anti-zero is an important information for structural control. Conventionally, the dynamic

0022-460X/01/400877 + 23 $35.00/0 

TABLE 1

*The relationship between finite-element and boundary-element methods in deriving dynamic stiffness and flexibility matrices*

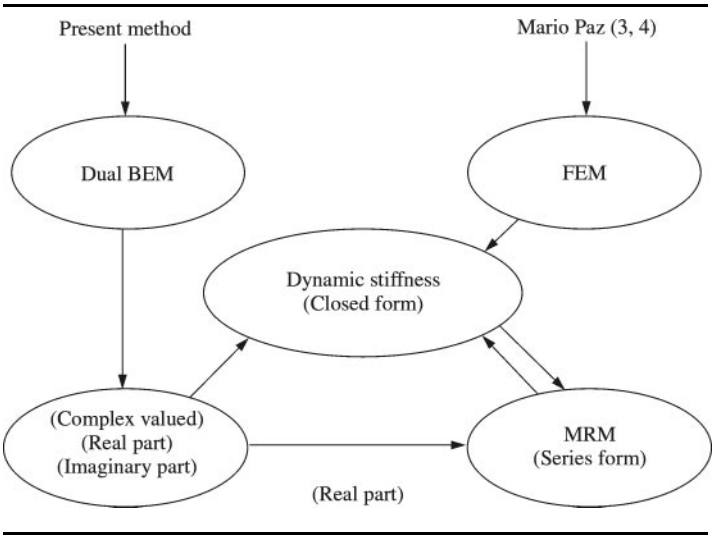


stiffness was determined by using the complex-valued BEM. Recently, Chen and his coworkers developed the real-part BEM [15, 16], the imaginary-part BEM [17] and the multiple reciprocity method [18] to solve the Helmholtz eigenproblem. Although spurious solutions appear, they can be filtered out by using some techniques, e.g., residue method [18–20], singular-value decomposition (SVD) [6, 21], generalized singular-value decomposition (GSVD) [22], CHEEF method [23] and domain partition technique [17]. Whether the real- or the imaginary-part BEM can be applied to determine the stiffness and flexibility in half effort or not is the main concern of the present paper. Also, the derivation of static flexibility for free–free structure by finding the inverse of a singular stiffness matrix will be addressed.

In this paper, we will construct the dynamic stiffness and dynamic flexibility by using two approaches, the real- and the imaginary-part BEMs. All the influence matrices for the three cases, a rod, a beam and a circular membrane, have the same mathematical structures, which can be decomposed into two parts: true and spurious poles using the singular-value decomposition. The spurious eigensolutions encountered in the real- or the imaginary-part formulations can be filtered out at the same time in constructing the dynamic stiffness and dynamic flexibility matrices, since the spurious part can be cancelled out analytically. The results using the real- and imaginary-part BEMs will be compared with each other. Also, the true eigenvalues can be directly found in the boundary dynamic stiffness or flexibility without the problem of spurious solution. The static flexibility will be determined from the static stiffness by using truncated singular-value decomposition [24] or pseudo-inverse [25].

## 2. METHODS FOR DERIVING DYNAMIC BOUNDARY STIFFNESS AND BOUNDARY FLEXIBILITY MATRICES OF A ROD

The governing equation for a unit-length rod is

$$\frac{\mathrm{d}^2 u(x)}{\mathrm{d}x^2} + k^2 u(x) = 0, \quad 0 < x < 1, \tag{1}$$

where $u$ is the axial displacement at the location $x$, $k^2 = \rho\omega^2/EA$, in which $\rho$ is the density, $\omega$ the angular frequency, $A$ the area of cross-section and $E$ the Young's modulus. By using Green's third identity, we can derive the singular ($UT$) integral equation and hypersingular ($LM$) integral equation. By moving the field point to the boundary, we have [21]

*Real-part UT equation* ($U_R\underset{\sim}{t} = T_R\underset{\sim}{u}$):

$$\begin{bmatrix} \frac{-1}{\sqrt{2}} & \frac{-1}{\sqrt{2}} \\ \frac{1}{\sqrt{2}} & \frac{-1}{\sqrt{2}} \end{bmatrix} \begin{bmatrix} \cos\frac{k}{2} & 0 \\ 0 & \sin\frac{k}{2} \end{bmatrix} \begin{bmatrix} \sin\frac{k}{2} & 0 \\ 0 & \cos\frac{k}{2} \end{bmatrix} \begin{bmatrix} \frac{-1}{\sqrt{2}} & \frac{1}{\sqrt{2}} \\ \frac{-1}{\sqrt{2}} & \frac{-1}{\sqrt{2}} \end{bmatrix} \begin{Bmatrix} t(0) \\ t(1) \end{Bmatrix}$$

$$= -k \begin{bmatrix} \frac{-1}{\sqrt{2}} & \frac{-1}{\sqrt{2}} \\ \frac{1}{\sqrt{2}} & \frac{-1}{\sqrt{2}} \end{bmatrix} \begin{bmatrix} \sin\frac{k}{2} & 0 \\ 0 & \cos\frac{k}{2} \end{bmatrix} \begin{bmatrix} \sin\frac{k}{2} & 0 \\ 0 & \cos\frac{k}{2} \end{bmatrix} \begin{bmatrix} \frac{-1}{\sqrt{2}} & \frac{1}{\sqrt{2}} \\ \frac{-1}{\sqrt{2}} & \frac{-1}{\sqrt{2}} \end{bmatrix} \begin{Bmatrix} u(0) \\ u(1) \end{Bmatrix}, \tag{2}$$

where $t(x) = \mathrm{d}u(x)/\mathrm{d}x$.

*Real-part LM equation* ($L_R\underset{\sim}{t} = M_R\underset{\sim}{u}$):

$$\begin{bmatrix} \frac{-1}{\sqrt{2}} & \frac{-1}{\sqrt{2}} \\ \frac{1}{\sqrt{2}} & \frac{-1}{\sqrt{2}} \end{bmatrix} \begin{bmatrix} \sin\frac{k}{2} & 0 \\ 0 & \cos\frac{k}{2} \end{bmatrix} \begin{bmatrix} \sin\frac{k}{2} & 0 \\ 0 & \cos\frac{k}{2} \end{bmatrix} \begin{bmatrix} \frac{-1}{\sqrt{2}} & \frac{1}{\sqrt{2}} \\ \frac{-1}{\sqrt{2}} & \frac{-1}{\sqrt{2}} \end{bmatrix} \begin{Bmatrix} t(0) \\ t(1) \end{Bmatrix}$$

$$= -k \begin{bmatrix} \frac{-1}{\sqrt{2}} & \frac{-1}{\sqrt{2}} \\ \frac{1}{\sqrt{2}} & \frac{-1}{\sqrt{2}} \end{bmatrix} \begin{bmatrix} \sin\frac{k}{2} & 0 \\ 0 & \cos\frac{k}{2} \end{bmatrix} \begin{bmatrix} \cos\frac{k}{2} & 0 \\ 0 & \sin\frac{k}{2} \end{bmatrix} \begin{bmatrix} \frac{-1}{\sqrt{2}} & \frac{1}{\sqrt{2}} \\ \frac{-1}{\sqrt{2}} & \frac{-1}{\sqrt{2}} \end{bmatrix} \begin{Bmatrix} u(0) \\ u(1) \end{Bmatrix}. \tag{3}$$

*Imaginary-part UT equation* ($U_I\underset{\sim}{t} = T_I\underset{\sim}{u}$):

$$\begin{bmatrix} \frac{-1}{\sqrt{2}} & \frac{-1}{\sqrt{2}} \\ \frac{1}{\sqrt{2}} & \frac{-1}{\sqrt{2}} \end{bmatrix} \begin{bmatrix} \sin\frac{k}{2} & 0 \\ 0 & \cos\frac{k}{2} \end{bmatrix} \begin{bmatrix} \sin\frac{k}{2} & 0 \\ 0 & \cos\frac{k}{2} \end{bmatrix} \begin{bmatrix} \frac{-1}{\sqrt{2}} & \frac{1}{\sqrt{2}} \\ \frac{-1}{\sqrt{2}} & \frac{-1}{\sqrt{2}} \end{bmatrix} \begin{Bmatrix} t(0) \\ t(1) \end{Bmatrix}$$

$$= -k \begin{bmatrix} \frac{-1}{\sqrt{2}} & \frac{-1}{\sqrt{2}} \\ \frac{1}{\sqrt{2}} & \frac{-1}{\sqrt{2}} \end{bmatrix} \begin{bmatrix} \sin\frac{k}{2} & 0 \\ 0 & \cos\frac{k}{2} \end{bmatrix} \begin{bmatrix} \cos\frac{k}{2} & 0 \\ 0 & \sin\frac{k}{2} \end{bmatrix} \begin{bmatrix} \frac{-1}{\sqrt{2}} & \frac{1}{\sqrt{2}} \\ \frac{-1}{\sqrt{2}} & \frac{-1}{\sqrt{2}} \end{bmatrix} \begin{Bmatrix} u(0) \\ u(1) \end{Bmatrix}. \tag{4}$$

*Imaginary-part LM equation* ($L_I \underset{\sim}{t} = M_I \underset{\sim}{u}$):

$$\begin{bmatrix} \frac{-1}{\sqrt{2}} & \frac{-1}{\sqrt{2}} \\ \frac{1}{\sqrt{2}} & \frac{-1}{\sqrt{2}} \end{bmatrix} \begin{bmatrix} \cos\frac{k}{2} & 0 \\ 0 & \sin\frac{k}{2} \end{bmatrix} \begin{bmatrix} \sin\frac{k}{2} & 0 \\ 0 & \cos\frac{k}{2} \end{bmatrix} \begin{bmatrix} \frac{-1}{\sqrt{2}} & \frac{1}{\sqrt{2}} \\ \frac{-1}{\sqrt{2}} & \frac{-1}{\sqrt{2}} \end{bmatrix} \begin{Bmatrix} t(0) \\ t(1) \end{Bmatrix}$$

$$= k \begin{bmatrix} \frac{-1}{\sqrt{2}} & \frac{-1}{\sqrt{2}} \\ \frac{1}{\sqrt{2}} & \frac{-1}{\sqrt{2}} \end{bmatrix} \begin{bmatrix} \cos\frac{k}{2} & 0 \\ 0 & \sin\frac{k}{2} \end{bmatrix} \begin{bmatrix} \cos\frac{k}{2} & 0 \\ 0 & \sin\frac{k}{2} \end{bmatrix} \begin{bmatrix} \frac{-1}{\sqrt{2}} & \frac{1}{\sqrt{2}} \\ \frac{-1}{\sqrt{2}} & \frac{-1}{\sqrt{2}} \end{bmatrix} \begin{Bmatrix} u(0) \\ u(1) \end{Bmatrix}. \tag{5}$$

By combining the real and imaginary parts together, the complex-valued dual equations can be obtained without any difficulty. For the sake of comparisons in the mathematical structures for the matrices, equations (2)–(5) can be rewritten as

*Real-part UT equation*:

$$[\Phi][D^1][D^2][\Phi]^{-1} \underset{\sim}{t} = k[\Phi][D^2][D^2][\Phi]^{-1} \underset{\sim}{u}, \tag{6}$$

*Real-part LM equation*:

$$[\Phi][D^2][D^2][\Phi]^{-1} \underset{\sim}{t} = k[\Phi][D^2][D^1][\Phi]^{-1} \underset{\sim}{u}, \tag{7}$$

*Imaginary-part UT equation*:

$$[\Phi][D^2][D^2][\Phi]^{-1} \underset{\sim}{t} = k[\Phi][D^2][D^1][\Phi]^{-1} \underset{\sim}{u}, \tag{8}$$

*Imaginary-part LM equation*:

$$[\Phi][D^1][D^2][\Phi]^{-1} \underset{\sim}{t} = -k[\Phi][D^1][D^1][\Phi]^{-1} \underset{\sim}{u}, \tag{9}$$

where

$$[\Phi] = \begin{bmatrix} \frac{-1}{\sqrt{2}} & \frac{-1}{\sqrt{2}} \\ \frac{1}{\sqrt{2}} & \frac{-1}{\sqrt{2}} \end{bmatrix}, \tag{10}$$

$$[D^1] = \begin{bmatrix} \cos\frac{k}{2} & 0 \\ 0 & \sin\frac{k}{2} \end{bmatrix}, \qquad [D^2] = \begin{bmatrix} \sin\frac{k}{2} & 0 \\ 0 & \cos\frac{k}{2} \end{bmatrix}, \tag{11, 12}$$

$$\underset{\sim}{u} = \begin{Bmatrix} u(0) \\ u(1) \end{Bmatrix}, \qquad \underset{\sim}{t} = \begin{Bmatrix} t(0) \\ t(1) \end{Bmatrix}. \tag{13, 14}$$

It is interesting to summarize all the results of equations (6)–(9) in Figure 1. The general formula can be represented by

$$[\Phi][D_A^s][D_A^t][\Phi]^{-1} \underset{\sim}{u} = [\Phi][D_B^s][D_B^t][\Phi]^{-1} \underset{\sim}{t}, \tag{15}$$

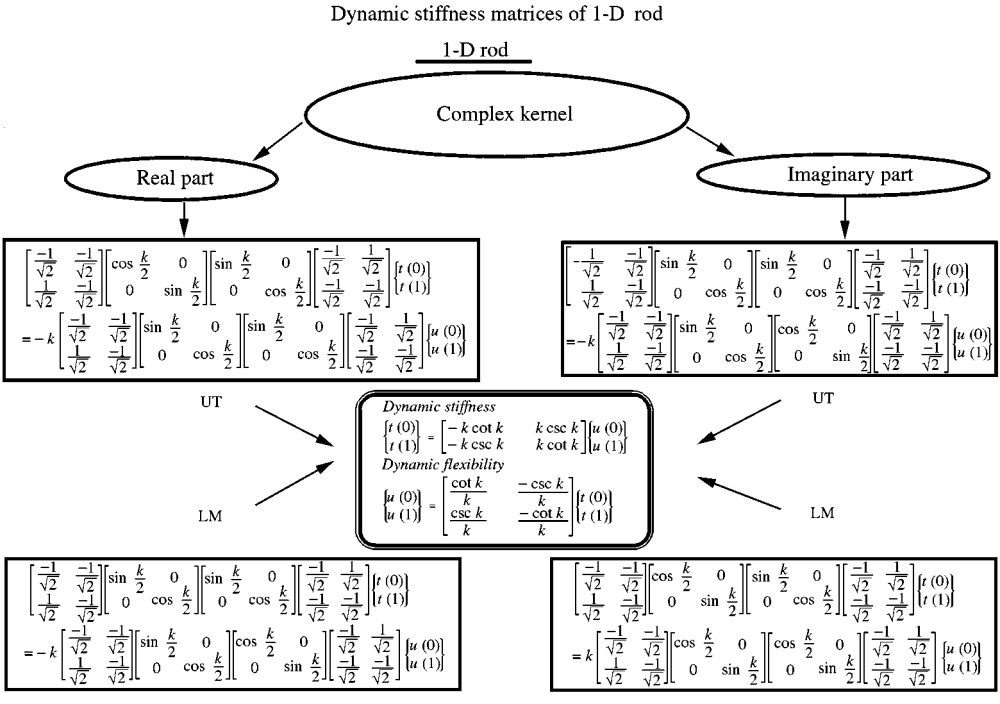


Figure 1. Dynamic stiffness and flexibility matrices for a rod using the dual formulations.

where the subscripts $A$ and $B$ can be either $[T]$, and $[U]$, or $[M]$, and $[L]$ and the superscripts $s$ and $t$ denote spurious and true respectively. The true eigenvalues occur when $\det[D_A^t] = 0$ for the Neumann problem, while the spurious eigenvalues occur when $\det[D_A^s] = 0$. For the Dirichlet problem, the true eigenvalues occur when $\det[D_B^t] = 0$, the spurious eigenvalues occur when $\det[D_B^s] = 0$. The true and spurious boundary modes can be determined from the column vectors of $\Phi$. The dynamic stiffness matrix can be obtained by

$$[K] = [U]^{-1}[T] = [L]^{-1}[M], \tag{16}$$

where $U$ can be $U_R$ (or $U_I$), $T$ can be $T_R$ (or $T_I$), $L$ can be $L_R$ (or $L_I$), $M$ can be $M_R$ (or $M_I$), and $\underset{\sim}{t} = [K]\underset{\sim}{u}$ as shown below:

$$\begin{Bmatrix} t(0) \\ t(1) \end{Bmatrix} = \begin{bmatrix} -k\cot(k) & k\csc(k) \\ -k\csc(k) & k\cot(k) \end{bmatrix} \begin{Bmatrix} u(0) \\ u(1) \end{Bmatrix}. \tag{17}$$

The dynamic stiffness $k_{11}$ versus $k$ is shown in Figure 2, where the peak indicates the true eigenvalue. Similarly, the dynamic flexibility matrix can be expressed as

$$[F] = [T]^{-1}[U] = [M]^{-1}[L], \tag{18}$$

where $\underset{\sim}{u} = [F]\underset{\sim}{t}$ is shown below:

$$\begin{Bmatrix} u(0) \\ u(1) \end{Bmatrix} = \begin{bmatrix} \dfrac{\cot(k)}{k} & \dfrac{-\csc(k)}{k} \\ \dfrac{\csc(k)}{k} & \dfrac{-\cot(k)}{k} \end{bmatrix} \begin{Bmatrix} t(0) \\ t(1) \end{Bmatrix}. \tag{19}$$

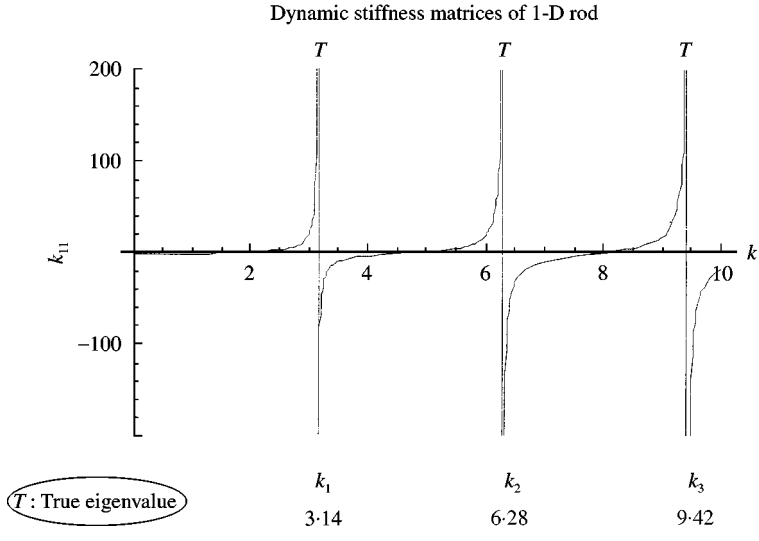


Figure 2. The dynamic stiffness $k_{11}$ versus $k$.

## 3. DETECTION OF TRUE AND SPURIOUS EIGENSOLUTIONS USING THE DUAL BEM IN CONJUNCTION WITH THE SINGULAR-VALUE DECOMPOSITION TECHNIQUE

By employing the SVD technique, we can transform the real-part $UT$ equation

$$[T_R]\,\underset{\sim}{u} = [U_R]\,\underset{\sim}{t} \tag{20}$$

into

$$\Phi_T \Sigma_T \Phi_T^{\mathrm{T}} \underset{\sim}{u} = \Phi_U \Sigma_U \Phi_U^{\mathrm{T}} \underset{\sim}{t}. \tag{21}$$

Similarly, the real-part $LM$ equation

$$[M_R]\,\underset{\sim}{u} = [L_R]\,\underset{\sim}{t} \tag{22}$$

can be rewritten as

$$\Phi_M \Sigma_M \Psi_M^{\mathrm{T}} \underset{\sim}{u} = \Phi_L \Sigma_L \Psi_L^{\mathrm{T}} \underset{\sim}{t}. \tag{23}$$

When $k$ is the first true eigenvalue of $\pi$, equations (2)–(5) turn out to be

*Real-part UT equation*:

$$\begin{bmatrix} -\frac{\sqrt{2}}{2} & -\frac{\sqrt{2}}{2} \\ -\frac{\sqrt{2}}{2} & \frac{\sqrt{2}}{2} \end{bmatrix} \begin{bmatrix} 1 & 0 \\ 0 & 0 \end{bmatrix} \begin{bmatrix} -\frac{\sqrt{2}}{2} & -\frac{\sqrt{2}}{2} \\ -\frac{\sqrt{2}}{2} & \frac{\sqrt{2}}{2} \end{bmatrix} \underset{\sim}{u}$$

$$= \begin{bmatrix} -\frac{\sqrt{2}}{2} & -\frac{\sqrt{2}}{2} \\ -\frac{\sqrt{2}}{2} & \frac{\sqrt{2}}{2} \end{bmatrix} \begin{bmatrix} 0 & 0 \\ 0 & 0 \end{bmatrix} \begin{bmatrix} -\frac{\sqrt{2}}{2} & -\frac{\sqrt{2}}{2} \\ -\frac{\sqrt{2}}{2} & \frac{\sqrt{2}}{2} \end{bmatrix} \underset{\sim}{t}. \tag{24}$$

*Real-part LM equation*:

$$\begin{bmatrix} -\frac{\sqrt{2}}{2} & -\frac{\sqrt{2}}{2} \\ -\frac{\sqrt{2}}{2} & \frac{\sqrt{2}}{2} \end{bmatrix} \begin{bmatrix} 0 & 0 \\ 0 & 0 \end{bmatrix} \begin{bmatrix} -\frac{\sqrt{2}}{2} & -\frac{\sqrt{2}}{2} \\ -\frac{\sqrt{2}}{2} & \frac{\sqrt{2}}{2} \end{bmatrix} \underset{\sim}{u}$$

$$= \begin{bmatrix} -\frac{\sqrt{2}}{2} & -\frac{\sqrt{2}}{2} \\ -\frac{\sqrt{2}}{2} & \frac{\sqrt{2}}{2} \end{bmatrix} \begin{bmatrix} 1 & 0 \\ 0 & 0 \end{bmatrix} \begin{bmatrix} -\frac{\sqrt{2}}{2} & -\frac{\sqrt{2}}{2} \\ -\frac{\sqrt{2}}{2} & \frac{\sqrt{2}}{2} \end{bmatrix} \underset{\sim}{t}. \tag{25}$$

*Imaginary-part UT equation*:

$$\begin{bmatrix} -\frac{\sqrt{2}}{2} & -\frac{\sqrt{2}}{2} \\ -\frac{\sqrt{2}}{2} & \frac{\sqrt{2}}{2} \end{bmatrix} \begin{bmatrix} 0 & 0 \\ 0 & 0 \end{bmatrix} \begin{bmatrix} -\frac{\sqrt{2}}{2} & -\frac{\sqrt{2}}{2} \\ -\frac{\sqrt{2}}{2} & \frac{\sqrt{2}}{2} \end{bmatrix} \underset{\sim}{u}$$

$$= \begin{bmatrix} -\frac{\sqrt{2}}{2} & \frac{\sqrt{2}}{2} \\ \frac{\sqrt{2}}{2} & \frac{\sqrt{2}}{2} \end{bmatrix} \begin{bmatrix} 0{\cdot}32 & 0 \\ 0 & 0 \end{bmatrix} \begin{bmatrix} \frac{\sqrt{2}}{2} & \frac{\sqrt{2}}{2} \\ -\frac{\sqrt{2}}{2} & \frac{\sqrt{2}}{2} \end{bmatrix} \underset{\sim}{t}. \tag{26}$$

*Imaginary-part LM equation*:

$$\begin{bmatrix} \frac{\sqrt{2}}{2} & -\frac{\sqrt{2}}{2} \\ -\frac{\sqrt{2}}{2} & -\frac{\sqrt{2}}{2} \end{bmatrix} \begin{bmatrix} 3{\cdot}14 & 0 \\ 0 & 0 \end{bmatrix} \begin{bmatrix} \frac{\sqrt{2}}{2} & \frac{\sqrt{2}}{2} \\ -\frac{\sqrt{2}}{2} & \frac{\sqrt{2}}{2} \end{bmatrix} \underset{\sim}{u}$$

$$= \begin{bmatrix} -\frac{\sqrt{2}}{2} & -\frac{\sqrt{2}}{2} \\ -\frac{\sqrt{2}}{2} & \frac{\sqrt{2}}{2} \end{bmatrix} \begin{bmatrix} 0 & 0 \\ 0 & 0 \end{bmatrix} \begin{bmatrix} -\frac{\sqrt{2}}{2} & -\frac{\sqrt{2}}{2} \\ -\frac{\sqrt{2}}{2} & \frac{\sqrt{2}}{2} \end{bmatrix} \underset{\sim}{t}. \tag{27}$$

All the interesting results including the true and spurious eigensolutions for the Dirichlet and Neumann problems are shown in Table 2. For the problem of mixed-type boundary condition, we have the $UT$ equation in the form

$$[A]\underset{\sim}{x} = [B]\underset{\sim}{y}, \tag{28}$$

TABLE 2

*True and spurious eigensystems for the Dirichlet and Neumann problems using the singular-value decomposition technique*

| | Exact solution | Real-part $UT$ method | Real-part $LM$ method | Imag-part $UT$ method | Imag-part $LM$ method |
|---|---|---|---|---|---|
| Dirichlet problem | Eigenvalue $\lambda_1 = \pi$ | $\pi$ | $\pi$ | $\pi$ | $\pi$ |
| | Eigenvector $\underset{\sim}{\psi}_1 = \begin{bmatrix} 1 \\ -1 \end{bmatrix}$ | Failure | $\underset{\sim}{\psi}_D = \begin{bmatrix} -\frac{\sqrt{2}}{2} \\ \frac{\sqrt{2}}{2} \end{bmatrix}$ $\underset{\sim}{\Psi}_D = \begin{bmatrix} -\frac{\sqrt{2}}{2} \\ \frac{\sqrt{2}}{2} \end{bmatrix}$ | Failure | |
| Neumann problem | Eigenvalue $\lambda_1 = \pi$ | $\pi$ | $\pi$ | $\pi$ | $\pi$ |
| | Eigenvector $\underset{\sim}{\psi}_1 = \begin{bmatrix} 1 \\ -1 \end{bmatrix}$ $\underset{\sim}{\psi}_N = \begin{bmatrix} -\frac{\sqrt{2}}{2} \\ \frac{\sqrt{2}}{2} \end{bmatrix}$ | Failure | Failure | $\underset{\sim}{\psi}_N = \begin{bmatrix} -\frac{\sqrt{2}}{2} \\ \frac{\sqrt{2}}{2} \end{bmatrix}$ | |

where

$$\underset{\sim}{x} = \begin{bmatrix} u(0) \\ -t(1) \end{bmatrix}, \qquad \underset{\sim}{y} = \begin{bmatrix} u(1) \\ t(0) \end{bmatrix}. \tag{29, 30}$$

By employing the SVD technique, equation (28) reduces to

$$\Phi_A \Sigma_A \Psi_A^{\mathrm{T}} \underset{\sim}{x} = \Phi_B \Sigma_B \Psi_B^{\mathrm{T}} \underset{\sim}{y}. \tag{31}$$

Similarly, we can obtain the $LM$ equation,

$$[C]\underset{\sim}{x} = [D]\underset{\sim}{y}. \tag{32}$$

By employing the SVD technique, equation (32) reduces to

$$\Phi_C \Sigma_C \Psi_C^{\mathrm{T}} \underset{\sim}{x} = \Phi_D \Sigma_D \Psi_D^{\mathrm{T}} \underset{\sim}{y}. \tag{33}$$

When $k$ is the first true eigenvalue of $\pi/2$, equations (31) and (33) reduce to

*Real-part UT equation*:

$$\begin{bmatrix} -1 & 0 \\ 0 & 1 \end{bmatrix} \begin{bmatrix} 0{\cdot}59 & 0 \\ 0 & 0 \end{bmatrix} \begin{bmatrix} 0{\cdot}84 & 0{\cdot}54 \\ -0{\cdot}54 & -0{\cdot}84 \end{bmatrix} \underset{\sim}{x}$$
$$= \begin{bmatrix} 0 & -1 \\ -1 & 0 \end{bmatrix} \begin{bmatrix} 0{\cdot}59 & 0 \\ 0 & 0 \end{bmatrix} \begin{bmatrix} -0{\cdot}84 & 0{\cdot}54 \\ 0{\cdot}54 & 0{\cdot}84 \end{bmatrix} \underset{\sim}{y}. \tag{34}$$

*Real-part LM equation*:

$$\begin{bmatrix} 0 & -1 \\ -1 & 0 \end{bmatrix}\begin{bmatrix} 0{\cdot}94 & 0 \\ 0 & 0 \end{bmatrix}\begin{bmatrix} -0{\cdot}84 & 0{\cdot}54 \\ 0{\cdot}54 & 0{\cdot}84 \end{bmatrix}\underset{\sim}{x}$$
$$= \begin{bmatrix} -1 & 0 \\ 0 & 1 \end{bmatrix}\begin{bmatrix} 0{\cdot}94 & 0 \\ 0 & 0 \end{bmatrix}\begin{bmatrix} -0{\cdot}84 & 0{\cdot}54 \\ 0{\cdot}54 & 0{\cdot}84 \end{bmatrix}\underset{\sim}{y}. \tag{35}$$

Similarly, we have

*Imaginary-part UT equation*:

$$\begin{bmatrix} 0 & -1 \\ -1 & 0 \end{bmatrix}\begin{bmatrix} 0{\cdot}59 & 0 \\ 0 & 0 \end{bmatrix}\begin{bmatrix} -0{\cdot}84 & 0{\cdot}54 \\ 0{\cdot}54 & 0{\cdot}84 \end{bmatrix}\underset{\sim}{x}$$
$$= \begin{bmatrix} -1 & 0 \\ 0 & 1 \end{bmatrix}\begin{bmatrix} 0{\cdot}59 & 0 \\ 0 & 0 \end{bmatrix}\begin{bmatrix} 0{\cdot}84 & -0{\cdot}54 \\ 0{\cdot}54 & 0{\cdot}84 \end{bmatrix}\underset{\sim}{y}. \tag{36}$$

*Imaginary-part LM equation*:

$$\begin{bmatrix} -1 & 0 \\ 0 & 1 \end{bmatrix}\begin{bmatrix} 0{\cdot}94 & 0 \\ 0 & 0 \end{bmatrix}\begin{bmatrix} 0{\cdot}84 & -0{\cdot}54 \\ -0{\cdot}54 & -0{\cdot}84 \end{bmatrix}\underset{\sim}{x}$$
$$= \begin{bmatrix} 0 & -1 \\ -1 & 0 \end{bmatrix}\begin{bmatrix} 0{\cdot}94 & 0 \\ 0 & 0 \end{bmatrix}\begin{bmatrix} 0{\cdot}84 & -0{\cdot}54 \\ 0{\cdot}54 & 0{\cdot}84 \end{bmatrix}\underset{\sim}{y}. \tag{37}$$

When $k$ is the first spurious eigenvalue of $\pi$, equations (31) and (33) reduce to

*Real-part UT equation*:

$$\begin{bmatrix} -0{\cdot}707 & -0{\cdot}707 \\ -0{\cdot}707 & 0{\cdot}707 \end{bmatrix}\begin{bmatrix} 0{\cdot}707 & 0 \\ 0 & 0 \end{bmatrix}\begin{bmatrix} 1 & 0 \\ 0 & 1 \end{bmatrix}\underset{\sim}{x}$$
$$= \begin{bmatrix} -0{\cdot}707 & -0{\cdot}707 \\ -0{\cdot}707 & 0{\cdot}707 \end{bmatrix}\begin{bmatrix} 0{\cdot}707 & 0 \\ 0 & 0 \end{bmatrix}\begin{bmatrix} -1 & 0 \\ 0 & 1 \end{bmatrix}\underset{\sim}{y}. \tag{38}$$

*Real-part LM equation*:

$$\begin{bmatrix} -0{\cdot}707 & -0{\cdot}707 \\ -0{\cdot}707 & 0{\cdot}707 \end{bmatrix}\begin{bmatrix} 0{\cdot}707 & 0 \\ 0 & 0 \end{bmatrix}\begin{bmatrix} 0 & 1 \\ -1 & 0 \end{bmatrix}\underset{\sim}{x}$$
$$= \begin{bmatrix} -0{\cdot}707 & 0{\cdot}707 \\ -0{\cdot}707 & -0{\cdot}707 \end{bmatrix}\begin{bmatrix} 0{\cdot}707 & 0 \\ 0 & 0 \end{bmatrix}\begin{bmatrix} 0 & 1 \\ -1 & 0 \end{bmatrix}\underset{\sim}{y}. \tag{39}$$

Similarly, the imaginary-part $UT$ and $LM$ equations can be derived, respectively, as follows:

$$\begin{bmatrix} -0{\cdot}707 & -0{\cdot}707 \\ 0{\cdot}707 & -0{\cdot}707 \end{bmatrix}\begin{bmatrix} 0{\cdot}23 & 0 \\ 0 & 0 \end{bmatrix}\begin{bmatrix} 0 & -1 \\ -1 & 0 \end{bmatrix}\underset{\sim}{x}$$
$$= \begin{bmatrix} -0{\cdot}303 & -0{\cdot}952 \\ 0{\cdot}952 & -0{\cdot}303 \end{bmatrix}\begin{bmatrix} 0{\cdot}524 & 0 \\ 0 & 0 \end{bmatrix}\begin{bmatrix} 0 & -1 \\ 1 & 0 \end{bmatrix}\underset{\sim}{y}. \tag{40}$$

$$\begin{bmatrix} -0{\cdot}707 & 0{\cdot}707 \\ 0{\cdot}707 & 0{\cdot}707 \end{bmatrix}\begin{bmatrix} 2{\cdot}22 & 0 \\ 0 & 0 \end{bmatrix}\begin{bmatrix} 1 & 0 \\ 0 & 1 \end{bmatrix}\underset{\sim}{x}$$
$$= \begin{bmatrix} -0{\cdot}707 & 0{\cdot}707 \\ 0{\cdot}707 & 0{\cdot}707 \end{bmatrix}\begin{bmatrix} 2{\cdot}22 & 0 \\ 0 & 0 \end{bmatrix}\begin{bmatrix} -1 & 0 \\ 0 & 1 \end{bmatrix}\underset{\sim}{y}. \tag{41}$$

All the interesting results including the true and spurious eigensolutions for the problem of mixed-type boundary condition are shown in Table 3. By using the SVD technique of updating terms [26], the true solution can be extracted out emerging as

$$\begin{bmatrix} U \\ L \end{bmatrix} \underset{\sim}{\psi}_D = 0, \tag{42}$$

or

$$\begin{bmatrix} T \\ M \end{bmatrix} \underset{\sim}{\psi}_N = 0, \tag{43}$$

where $\underset{\sim}{\psi}_D$ and $\underset{\sim}{\psi}_N$ are the true boundary modes for the Dirichlet and Neumann problems respectively. For the mixed-type boundary condition problem, the true boundary mode, $\underset{\sim}{\psi}$, can be obtained by combining

$$\begin{bmatrix} A \\ C \end{bmatrix} \underset{\sim}{\psi}_1 = 0, \tag{44}$$

or

$$\begin{bmatrix} B \\ D \end{bmatrix} \underset{\sim}{\psi}_2 = 0, \tag{45}$$

where $\underset{\sim}{\psi}_1$ and $\underset{\sim}{\psi}_2$ are the true boundary modes for the mixed-type problem using equations (44) and (45) respectively. All the interesting results are shown in Table 4.

In order to determine the spurious eigensolution, we can employ SVD technique of updating documents [26]

$$\underset{\sim}{\phi}_p^{\mathrm{T}} [U \;\; T] = 0. \tag{46}$$

After transposing equation (46), we have

$$\begin{bmatrix} U^{\mathrm{T}} \\ T^{\mathrm{T}} \end{bmatrix} \underset{\sim}{\phi}_p = 0. \tag{47}$$

Similarly, we have

$$\underset{\sim}{\phi}_s^{\mathrm{T}} [L \;\; M] = 0 \quad \text{or} \quad \begin{bmatrix} L^{\mathrm{T}} \\ M^{\mathrm{T}} \end{bmatrix} \underset{\sim}{\phi}_s = 0, \tag{48}$$

where $\underset{\sim}{\phi}_p$ and $\underset{\sim}{\phi}_s$ are the non-trivial spurious boundary modes encountered in the $UT$ and $LM$ equations respectively. For the mixed-type boundary condition problem, we have

$$\begin{bmatrix} A^{\mathrm{T}} \\ B^{\mathrm{T}} \end{bmatrix} \underset{\sim}{\phi}_1 = 0, \tag{49}$$

or

$$\begin{bmatrix} C^{\mathrm{T}} \\ D^{\mathrm{T}} \end{bmatrix} \underset{\sim}{\phi}_2 = 0, \tag{50}$$

where $\underset{\sim}{\phi}_1$ and $\underset{\sim}{\phi}_2$ are the non-trivial spurious boundary modes for the mixed-type problem using equations (49) and (50) respectively. All the interesting results are shown in Table 5.

TABLE 3

*True and spurious eigensystems for the mixed-type problems using the singular-value decomposition technique*

| | | Real $UT$ | Real $LM$ | Imag $UT$ | Imag $LM$ |
|---|---|---|---|---|---|
| Eigenvalue | True | $\frac{\pi}{2}$ | $\frac{\pi}{2}$ | $\frac{\pi}{2}$ | $\frac{\pi}{2}$ |
| | Spurious | $\pi$ | $\pi$ | $\pi$ | $\pi$ |
| Eigenvector | True | $\underset{\sim}{\psi}_1 = \begin{bmatrix} 0{\cdot}54 \\ 0{\cdot}84 \end{bmatrix}$ | $\underset{\sim}{\psi}_2 = \begin{bmatrix} 0{\cdot}54 \\ 0{\cdot}84 \end{bmatrix}$ | $\underset{\sim}{\psi}_1 = \begin{bmatrix} 0{\cdot}54 \\ 0{\cdot}84 \end{bmatrix}$ | $\underset{\sim}{\psi}_2 = \begin{bmatrix} 0{\cdot}54 \\ 0{\cdot}84 \end{bmatrix}$ |
| | Spurious | $\phi_1 = \begin{bmatrix} 0 \\ 1 \end{bmatrix}$ | $\phi_2 = \begin{bmatrix} 1 \\ 0 \end{bmatrix}$ | $\phi_1 = \begin{bmatrix} 1 \\ 0 \end{bmatrix}$ | $\phi_2 = \begin{bmatrix} 0 \\ 1 \end{bmatrix}$ |
| Exact eigenvalue | True | $\frac{(2n-1)\pi}{2}$ | $\frac{(2n-1)\pi}{2}$ | $\frac{(2n-1)\pi}{2}$ | $\frac{(2n-1)\pi}{2}$ |
| | Spurious | $n\pi$ | $n\pi$ | $n\pi$ | $n\pi$ |
| Exact eigenvector | True | $\psi_t = \begin{bmatrix} 1 \\ (-1)^n \frac{(2n-1)\pi}{2} \end{bmatrix}$ | $\psi_t = \begin{bmatrix} 1 \\ (-1)^n \frac{(2n-1)\pi}{2} \end{bmatrix}$ | $\psi_t = \begin{bmatrix} 1 \\ (-1)^n \frac{(2n-1)\pi}{2} \end{bmatrix}$ | $\psi_t = \begin{bmatrix} 1 \\ (-1)^n \frac{(2n-1)\pi}{2} \end{bmatrix}$ |
| | Spurious | $\phi_s = \begin{bmatrix} 0 \\ 1 \end{bmatrix}$ | $\phi_s = \begin{bmatrix} 0 \\ 1 \end{bmatrix}$ | $\phi_s = \begin{bmatrix} 0 \\ 1 \end{bmatrix}$ | $\phi_s = \begin{bmatrix} 0 \\ 1 \end{bmatrix}$ |

TABLE 4

*The occurring mechanism of true and spurious eigensystems for the Dirichlet and Neumann problems using the dual formulation*

| | Spurious eigensystem | True eigensystem |
|---|---|---|
| Real-part dual BEM | $U_R^{\mathrm{T}}(k_s)\underset{\sim}{\phi}_p = 0 \quad k_s = 3{\cdot}14$<br>$T_R^{\mathrm{T}}(k_s)\underset{\sim}{\phi}_p = 0 \quad \underset{\sim}{\phi}_p = \begin{bmatrix} \frac{\sqrt{2}}{2} \\ -\frac{\sqrt{2}}{2} \end{bmatrix}$<br>$\begin{bmatrix} U_R^{\mathrm{T}} \\ T_R^{\mathrm{T}} \end{bmatrix}\underset{\sim}{\phi}_p = 0$ | $U_R(k_t)\underset{\sim}{\psi}_D = 0 \quad k_t = 3{\cdot}14$<br>$L_R(k_t)\underset{\sim}{\psi}_D = 0 \quad \underset{\sim}{\psi}_D = \begin{bmatrix} \frac{\sqrt{2}}{2} \\ -\frac{\sqrt{2}}{2} \end{bmatrix}$<br>$\begin{bmatrix} U_R \\ T_R \end{bmatrix}\underset{\sim}{\psi}_D = 0$ |
| | $L_R^{\mathrm{T}}(k_s)\underset{\sim}{\phi}_s = 0 \quad k_s = 3{\cdot}14$<br>$M_R^{\mathrm{T}}(k_s)\underset{\sim}{\phi}_s = 0 \quad \underset{\sim}{\phi}_s = \begin{bmatrix} \frac{\sqrt{2}}{2} \\ -\frac{\sqrt{2}}{2} \end{bmatrix}$<br>$\begin{bmatrix} L_R^{\mathrm{T}} \\ M_R^{\mathrm{T}} \end{bmatrix}\underset{\sim}{\phi}_s = 0$ | $T_R(k_t)\underset{\sim}{\psi}_N = 0 \quad k_t = 3{\cdot}14$<br>$M_R(k_t)\underset{\sim}{\psi}_N = 0 \quad \underset{\sim}{\psi}_N = \begin{bmatrix} \frac{\sqrt{2}}{2} \\ -\frac{\sqrt{2}}{2} \end{bmatrix}$<br>$\begin{bmatrix} T_R \\ M_R \end{bmatrix}\underset{\sim}{\psi}_N = 0$ |
| Imaginary-part dual BEM | $U_I^{\mathrm{T}}(k_s)\underset{\sim}{\phi}_p = 0 \quad k_s = 3{\cdot}14$<br>$T_I^{\mathrm{T}}(k_s)\underset{\sim}{\phi}_p = 0 \quad \underset{\sim}{\phi}_p = \begin{bmatrix} \frac{\sqrt{2}}{2} \\ -\frac{\sqrt{2}}{2} \end{bmatrix}$<br>$\begin{bmatrix} U_I^{\mathrm{T}} \\ T_I^{\mathrm{T}} \end{bmatrix}\underset{\sim}{\phi}_p = 0$ | $U_I(k_t)\underset{\sim}{\psi}_D = 0 \quad k_t = 3{\cdot}14$<br>$L_I(k_t)\underset{\sim}{\psi}_D = 0 \quad \underset{\sim}{\psi}_D = \begin{bmatrix} \frac{\sqrt{2}}{2} \\ -\frac{\sqrt{2}}{2} \end{bmatrix}$<br>$\begin{bmatrix} U_I \\ L_I \end{bmatrix}\underset{\sim}{\psi}_D = 0$ |
| | $L_I^{\mathrm{T}}(k_s)\underset{\sim}{\phi}_s = 0 \quad k_s = 3{\cdot}14$<br>$M_I^{\mathrm{T}}(k_s)\underset{\sim}{\phi}_s = 0 \quad \underset{\sim}{\phi}_s = \begin{bmatrix} \frac{\sqrt{2}}{2} \\ -\frac{\sqrt{2}}{2} \end{bmatrix}$<br>$\begin{bmatrix} L_I^{\mathrm{T}} \\ M_I^{\mathrm{T}} \end{bmatrix}\underset{\sim}{\phi}_s = 0$ | $T_I(k_t)\underset{\sim}{\psi}_N = 0 \quad k_t = 3{\cdot}14$<br>$M_I(k_t)\underset{\sim}{\psi}_N = 0 \quad \underset{\sim}{\psi}_N = \begin{bmatrix} \frac{\sqrt{2}}{2} \\ -\frac{\sqrt{2}}{2} \end{bmatrix}$<br>$\begin{bmatrix} T_I \\ M_I \end{bmatrix}\underset{\sim}{\psi}_N = 0$ |

TABLE 5

*The occurring mechanism of true and spurious eigensystems for the mixed-type problems using the dual formulation*

| | Spurious eigensystem | | True eigensystem | |
|---|---|---|---|---|
| Real-part dual BEM | $A_R^{\mathrm{T}}(k_s)\underset{\sim}{\phi}_1 = 0$ | $k_s = 3{\cdot}14$ | $A_R(k_t)\underset{\sim}{\psi}_1 = 0$ | $k_t = 1{\cdot}57$ |
| | $B_R^{\mathrm{T}}(k_s)\underset{\sim}{\phi}_1 = 0$ | $\underset{\sim}{\phi}_1 = \begin{bmatrix}0\\1\end{bmatrix}$ | $C_R(k_t)\underset{\sim}{\psi}_1 = 0$ | $\underset{\sim}{\psi}_1 = \begin{bmatrix}0{\cdot}54\\0{\cdot}84\end{bmatrix}$ |
| | $\begin{bmatrix}A_R^{\mathrm{T}}\\B_R^{\mathrm{T}}\end{bmatrix}\underset{\sim}{\phi}_1 = 0$ | | $\begin{bmatrix}A_R\\C_R\end{bmatrix}\underset{\sim}{\psi}_1 = 0$ | |
| | $C_R^{\mathrm{T}}(k_s)\underset{\sim}{\phi}_2 = 0$ | $k_s = 3{\cdot}14$ | $B_R(k_t)\underset{\sim}{\psi}_2 = 0$ | $k_t = 1{\cdot}57$ |
| | $D_R^{\mathrm{T}}(k_s)\underset{\sim}{\phi}_2 = 0$ | $\underset{\sim}{\phi}_2 = \begin{bmatrix}1\\0\end{bmatrix}$ | $D_R(k_t)\underset{\sim}{\psi}_2 = 0$ | $\underset{\sim}{\psi}_2 = \begin{bmatrix}0{\cdot}54\\0{\cdot}84\end{bmatrix}$ |
| | $\begin{bmatrix}C_R^{\mathrm{T}}\\D_R^{\mathrm{T}}\end{bmatrix}\underset{\sim}{\phi}_2 = 0$ | | $\begin{bmatrix}B_R\\D_R\end{bmatrix}\underset{\sim}{\psi}_2 = 0$ | |
| Imaginary-part dual BEM | $A_I^{\mathrm{T}}(k_s)\underset{\sim}{\phi}_1 = 0$ | $k_s = 3{\cdot}14$ | $A_I(k_t)\underset{\sim}{\psi}_1 = 0$ | $k_t = 1{\cdot}57$ |
| | $B_I^{\mathrm{T}}(k_s)\underset{\sim}{\phi}_1 = 0$ | $\underset{\sim}{\phi}_1 = \begin{bmatrix}1\\0\end{bmatrix}$ | $C_I(k_t)\underset{\sim}{\psi}_1 = 0$ | $\underset{\sim}{\psi}_1 = \begin{bmatrix}0{\cdot}54\\0{\cdot}84\end{bmatrix}$ |
| | $\begin{bmatrix}A_I^{\mathrm{T}}\\B_I^{\mathrm{T}}\end{bmatrix}\underset{\sim}{\phi}_1 = 0$ | | $\begin{bmatrix}A_I\\C_I\end{bmatrix}\underset{\sim}{\psi}_1 = 0$ | |
| | $C_I^{\mathrm{T}}(k_s)\underset{\sim}{\phi}_2 = 0$ | $k_s = 3{\cdot}14$ | $B_I(k_t)\underset{\sim}{\psi}_2 = 0$ | $k_t = 1{\cdot}57$ |
| | $D_I^{\mathrm{T}}(k_s)\underset{\sim}{\phi}_2 = 0$ | $\underset{\sim}{\phi}_2 = \begin{bmatrix}0\\1\end{bmatrix}$ | $D_I(k_t)\underset{\sim}{\psi}_2 = 0$ | $\underset{\sim}{\psi}_2 = \begin{bmatrix}0{\cdot}54\\0{\cdot}84\end{bmatrix}$ |
| | $\begin{bmatrix}C_I^{\mathrm{T}}\\D_I^{\mathrm{T}}\end{bmatrix}\underset{\sim}{\phi}_2 = 0$ | | $\begin{bmatrix}B_I\\D_I\end{bmatrix}\underset{\sim}{\psi}_2 = 0$ | |

## 4. METHODS FOR DERIVING DYNAMIC BOUNDARY STIFFNESS AND DYNAMIC BOUNDARY FLEXIBILITY MATRICES OF A BEAM

For a unit-length beam, we have the governing equation

$$\frac{\mathrm{d}^4 u(x)}{\mathrm{d}x^4} - k^4 u(x) = 0, \quad 0 < x < 1, \tag{51}$$

where $u(x)$ is the lateral displacement and $k^4 = \rho\omega^2/EI$, in which $\rho$ is the mass per unit length and $I$ the moment of inertia. By using Green's third identity, we can find the $UT$ equation and $LM$ equation. Moving the field point close to the boundary, we have [6]

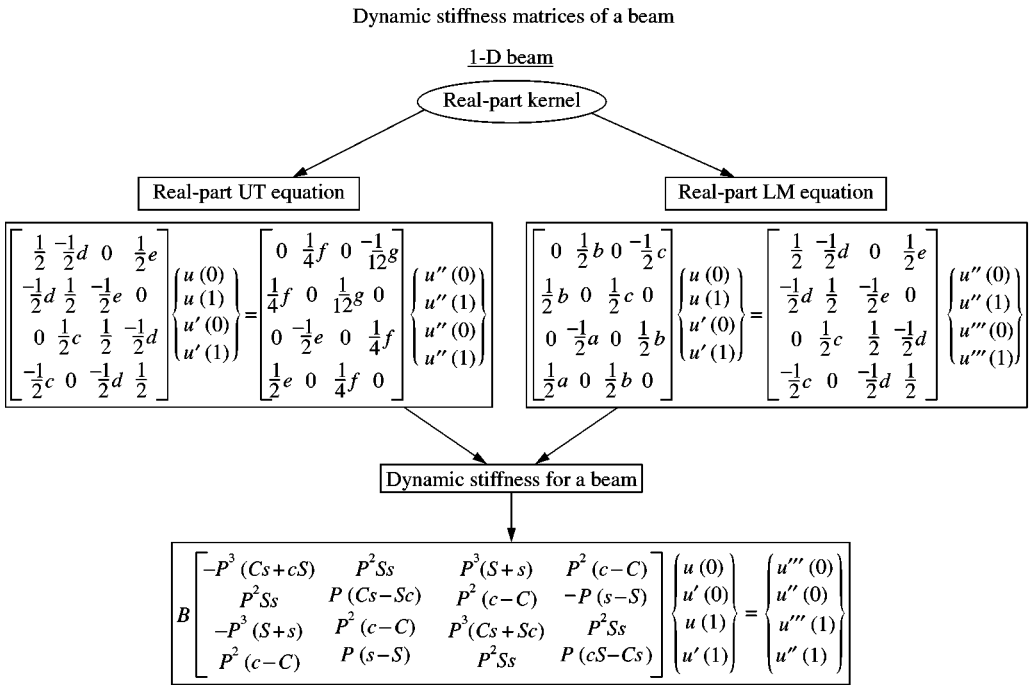


Figure 3. Dynamic stiffness and flexibility matrices for a beam using the dual formulation.

*Real-part UT equation* ($U\underset{\sim}{t} = T\underset{\sim}{u}$):

$$\begin{bmatrix} 0 & \frac{f}{4} & 0 & \frac{-g}{12} \\ \frac{f}{2} & 0 & \frac{g}{12} & 0 \\ 0 & \frac{-e}{2} & 0 & \frac{f}{4} \\ \frac{e}{2} & 0 & \frac{f}{4} & 0 \end{bmatrix} \begin{Bmatrix} u''(0) \\ u''(1) \\ u'''(0) \\ u'''(1) \end{Bmatrix} = \begin{bmatrix} \frac{1}{2} & \frac{-d}{2} & 0 & \frac{e}{2} \\ \frac{-d}{2} & \frac{1}{2} & \frac{-e}{12} & 0 \\ 0 & \frac{c}{2} & \frac{1}{2} & \frac{-d}{2} \\ \frac{-c}{2} & 0 & \frac{-d}{2} & \frac{1}{2} \end{bmatrix} \begin{Bmatrix} u(0) \\ u(1) \\ u'(0) \\ u'(1) \end{Bmatrix}, \tag{52}$$

where

$$a = \frac{k^3(\sinh(k)+\sin(k))}{2}, \qquad b = \frac{k^2(\cosh(k)-\cos(k))}{2}, \tag{53, 54}$$

$$c = \frac{k(\sinh(k)-\sin(k))}{2}, \qquad d = \frac{\cosh(k)+\cos(k)}{2}, \tag{55, 56}$$

$$e = \frac{\sinh(k)+\sin(k)}{2k}, \qquad f = \frac{\cosh(k)-\cos(k)}{k^2}, \tag{57, 58}$$

$$g = \frac{3(\sinh(k)-\sin(k))}{k^3}. \tag{59}$$

*Real-part LM equation* ($L\underset{\sim}{t} = M\underset{\sim}{u}$):

$$\begin{bmatrix} \frac{1}{2} & \frac{-d}{2} & 0 & \frac{e}{2} \\ \frac{-d}{2} & \frac{1}{2} & \frac{-e}{2} & 0 \\ 0 & \frac{c}{2} & \frac{1}{2} & \frac{-d}{2} \\ \frac{-c}{2} & 0 & \frac{-d}{2} & \frac{1}{2} \end{bmatrix} \begin{Bmatrix} u''(0) \\ u''(1) \\ u'''(0) \\ u'''(1) \end{Bmatrix} = \begin{bmatrix} 0 & \frac{b}{2} & 0 & \frac{-c}{2} \\ \frac{b}{2} & 0 & \frac{c}{2} & 0 \\ 0 & \frac{-a}{2} & 0 & \frac{b}{2} \\ \frac{a}{2} & 0 & \frac{b}{2} & 0 \end{bmatrix} \begin{Bmatrix} u(0) \\ u(1) \\ u'(0) \\ u'(1) \end{Bmatrix}. \tag{60}$$

It is interesting to summarize all the results of equations (52) and (60) in Figure 3. The dynamic stiffness matrix can be expressed as

$$[K] = [U]^{-1}[T], \tag{61}$$

where $[K]\underset{\sim}{u} = \underset{\sim}{t}$ is shown below:

$$B \begin{bmatrix} k^2Ss & k^2(c-C) & k(Cs-Sc) & -k(s-S) \\ k^2(c-C) & k^2Ss & k(s-S) & k(cS-Cs) \\ -k^3(Cs+cS) & k^3(S+s) & k^2Ss & k^2(c-C) \\ -k^3(S+s) & k^3(Cs+Sc) & k^2(c-C) & k^2Ss \end{bmatrix} \begin{Bmatrix} u(0) \\ u(1) \\ u'(0) \\ u'(1) \end{Bmatrix} = \begin{Bmatrix} u''(0) \\ u''(1) \\ u'''(0) \\ u'''(1) \end{Bmatrix}, \tag{62}$$

in which $S = \sinh(k)$, $s = \sin(k)$, $C = \cosh(k)$, $c = \cos(k)$ and $B = 1/(Cc - 1)$. By employing the *LM* formulation, we have

$$[K] = [L]^{-1}[M], \tag{63}$$

where $[K]\underset{\sim}{u} = \underset{\sim}{t}$ as shown below:

$$B \begin{bmatrix} k^2Ss & k^2(c-C) & k(Cs-Sc) & -k(s-S) \\ k^2(c-C) & k^2Ss & k(s-S) & k(cS-Cs) \\ -k^3(Cs+cS) & k^3(S+s) & k^2Ss & k^2(c-C) \\ -k^3(S+s) & k^3(Cs+Sc) & k^2(c-C) & k^2Ss \end{bmatrix} \begin{Bmatrix} u(0) \\ u(1) \\ u'(0) \\ u'(1) \end{Bmatrix} = \begin{Bmatrix} u''(0) \\ u''(1) \\ u'''(0) \\ u'''(1) \end{Bmatrix}. \tag{64}$$

It is interesting to find that the dynamic stiffness matrix derived by using the *UT* or *LM* method as shown in equations (62) and (64) are the same. To compare with the dynamic stiffness matrices using FEM [3], we can arrange the stiffness matrix in the following form:

$$B \begin{bmatrix} -k^3(Cs+cS) & k^2Ss & k^3(S+s) & k^2(c-C) \\ k^2Ss & k(Cs-Sc) & k^2(c-C) & -k(s-S) \\ -k^3(S+s) & k^2(c-C) & k^3(Cs+Sc) & k^2Ss \\ k^2(c-C) & k(s-S) & k^2Ss & k(cS-Cs) \end{bmatrix} \begin{Bmatrix} u(0) \\ u'(0) \\ u(1) \\ u'(1) \end{Bmatrix} = \begin{Bmatrix} u'''(0) \\ u''(0) \\ u'''(1) \\ u''(1) \end{Bmatrix}. \tag{65}$$

Also, we can rewrite equation (65) as

$$B \begin{bmatrix} -k^3(Cs+cS) & -k^2Ss & k^3(S+s) & -k^2(c-C) \\ -k^2Ss & k(cS-sC) & k^2(C-c) & k(s-S) \\ k^3(S+s) & k^2(C-c) & -k^3(Cs+Sc) & k^2Ss \\ k^2(C-c) & k(s-S) & k^2Ss & k(cS-Cs) \end{bmatrix} \begin{Bmatrix} \delta_1 \\ \theta_1 \\ \delta_2 \\ \theta_2 \end{Bmatrix} = \begin{Bmatrix} V_1 \\ M_1 \\ V_2 \\ M_2 \end{Bmatrix}, \tag{66}$$

where $u(0) = \delta_1$, $u(1) = \delta_2$, $u'(0) = -\theta_1$, $u'(1) = \theta_2$, $u'''(0) = V_1$, $u'''(1) = V_2$, $u''(0) = M_1$, $u''(1) = M_2$. It is interesting to find that equation (65) matches with the same result of equation (66) derived by Mario and Lam [3].

## 5. METHODS FOR DERIVING DYNAMIC STIFFNESS AND FLEXIBILITY MATRICES FOR A 2-D CIRCULAR MEMBRANE

For a circular membrane, the governing equation is the Helmholtz equation:

$$(\nabla^2 + k^2)u(x_1, x_2) = 0, \quad (x_1, x_2) \in D, \tag{67}$$

where $u$ is the lateral displacement, $k^2 = \rho\omega^2/T$, in which $\rho$ is the density, $T$ the tension, and $\nabla^2$ the Laplacian operator, $D$ the domain of the membrane. By using Green's third identity, we can find the $UT$ equation and $LM$ equation. Moving the field point to the boundary, we have

*Real-part UT equation* ($U\underset{\sim}{t} = T\underset{\sim}{u}$):

$$\mathbf{\Phi Y J \Phi}^{\mathrm{T}}\underset{\sim}{t} = k\mathbf{\Phi Y J}'\mathbf{\Phi}^{\mathrm{T}}\underset{\sim}{u}, \tag{68}$$

where

$$\mathbf{\Phi} = \begin{bmatrix}
1 & 1 & 0 & \cdots & 1 & 0 & 1 \\
1 & \cos\left(\frac{2\pi}{2N}\right) & \sin\left(\frac{2\pi}{2N}\right) & \vdots & \cos\left(\frac{2\pi(N-1)}{2N}\right) & \sin\left(\frac{2\pi(N-1)}{2N}\right) & \cos\left(\frac{2\pi N}{2N}\right) \\
1 & \cos\left(\frac{4\pi}{2N}\right) & \sin\left(\frac{4\pi}{2N}\right) & \vdots & \cos\left(\frac{4\pi(N-1)}{2N}\right) & \sin\left(\frac{4\pi(N-1)}{2N}\right) & \cos\left(\frac{4\pi N}{2N}\right) \\
\vdots & \vdots & \vdots & \vdots & \vdots & \vdots & \vdots \\
1 & \cos\left(\frac{2\pi(2N-2)}{2N}\right) & \sin\left(\frac{2\pi(2N-2)}{2N}\right) & \vdots & \cos\left(\frac{\pi(4N-4)(N-1)}{2N}\right) & \sin\left(\frac{\pi(4N-4)(N-1)}{2N}\right) & \cos\left(\frac{\pi(4N-4)(N)}{2N}\right) \\
1 & \cos\left(\frac{2\pi(2N-1)}{2N}\right) & \sin\left(\frac{2\pi(2N-1)}{2N}\right) & \vdots & \cos\left(\frac{\pi(4N-2)(N-1)}{2N}\right) & \sin\left(\frac{\pi(4N-2)(N-1)}{2N}\right) & \cos\left(\frac{\pi(4N-2)(N)}{2N}\right)
\end{bmatrix}_{2N\times 2N}, \tag{69}$$

$$\mathbf{J} = \begin{bmatrix}
\mathrm{J}_0(kr) & 0 & \cdots & \cdots & \cdots & \cdots & 0 \\
0 & \mathrm{J}_{-1}(kr) & 0 & \vdots & \vdots & \vdots & \vdots \\
\vdots & 0 & \mathrm{J}_1(kr) & 0 & \vdots & \vdots & \vdots \\
\vdots & \vdots & 0 & \ddots & 0 & \vdots & \vdots \\
\vdots & \vdots & \vdots & 0 & \mathrm{J}_{-(N-1)}(kr) & 0 & \vdots \\
\vdots & \vdots & \vdots & \vdots & 0 & \mathrm{J}_{N-1}(kr) & 0 \\
0 & 0 & 0 & \cdots & \cdots & 0 & \mathrm{J}_N(kr)
\end{bmatrix}_{2N\times 2N}, \tag{70}$$

$$\mathbf{Y} = \begin{bmatrix} \mathrm{Y}_0(kr) & 0 & \cdots & \cdots & \cdots & \cdots & 0 \\ 0 & \mathrm{Y}_{-1}(kr) & 0 & \vdots & \vdots & \vdots & \vdots \\ \vdots & 0 & \mathrm{Y}_1(kr) & 0 & \vdots & \vdots & \vdots \\ \vdots & \vdots & 0 & \ddots & 0 & \vdots & \vdots \\ \vdots & \vdots & \vdots & 0 & \mathrm{Y}_{-(N-1)}(kr) & 0 & \vdots \\ \vdots & \vdots & \vdots & \vdots & 0 & \mathrm{Y}_{N-1}(kr) & 0 \\ 0 & 0 & 0 & \cdots & \cdots & 0 & \mathrm{Y}_N(kr) \end{bmatrix}_{2N\times 2N}, \quad (71)$$

$$\mathbf{J}' = \begin{bmatrix} \mathrm{J}'_0(kr) & 0 & \cdots & \cdots & \cdots & \cdots & 0 \\ 0 & \mathrm{J}'_{-1}(kr) & 0 & \vdots & \vdots & \vdots & \vdots \\ \vdots & 0 & \mathrm{J}'_1(kr) & 0 & \vdots & \vdots & \vdots \\ \vdots & \vdots & 0 & \ddots & 0 & \vdots & \vdots \\ \vdots & \vdots & \vdots & 0 & \mathrm{J}'_{-(N-1)}(kr) & 0 & \vdots \\ \vdots & \vdots & \vdots & \vdots & 0 & \mathrm{J}'_{N-1}(kr) & 0 \\ 0 & 0 & 0 & \cdots & \cdots & 0 & \mathrm{J}'_N(kr) \end{bmatrix}_{2N\times 2N}, \quad (72)$$

in which $2N$ is the number of boundary elements, $\mathrm{J}_m$ and $\mathrm{Y}_m$ are the first and the second kind Bessel functions with order $m$, $\mathbf{\Phi}$ is the transformation matrix, $\underset{\sim}{u}$ the displacement vector and $\underset{\sim}{t}$ the normal flux vector. Similarly, we have

*Imaginary-part UT equation*:

$$\mathbf{\Phi J J \Phi}^{\mathrm{T}}\underset{\sim}{t} = k\mathbf{\Phi J J}'\mathbf{\Phi}^{\mathrm{T}}\underset{\sim}{u}. \quad (73)$$

*Real-part LM equation*:

$$\mathbf{\Phi Y}'\mathbf{J\Phi}^{\mathrm{T}}\underset{\sim}{t} = k\mathbf{\Phi Y}'\mathbf{J}'\mathbf{\Phi}^{\mathrm{T}}\underset{\sim}{u}, \quad (74)$$

where

$$\mathbf{Y}' = \begin{bmatrix} \mathrm{Y}'_0(kr) & 0 & \cdots & \cdots & \cdots & \cdots & 0 \\ 0 & \mathrm{Y}'_{-1}(kr) & 0 & \vdots & \vdots & \vdots & \vdots \\ \vdots & 0 & \mathrm{Y}'_1(kr) & 0 & \vdots & \vdots & \vdots \\ \vdots & \vdots & 0 & \ddots & 0 & \vdots & \vdots \\ \vdots & \vdots & \vdots & 0 & \mathrm{Y}'_{-(N-1)}(kr) & 0 & \vdots \\ \vdots & \vdots & \vdots & \vdots & 0 & \mathrm{Y}'_{N-1}(kr) & 0 \\ 0 & 0 & 0 & \cdots & \cdots & 0 & \mathrm{Y}'_N(kr) \end{bmatrix}_{2N\times 2N}, \quad (75)$$

*Imaginary-part LM equation*:

$$\mathbf{\Phi J}'\mathbf{J\Phi}^{\mathrm{T}}\underset{\sim}{t} = k\mathbf{\Phi J}'\mathbf{J}'\mathbf{\Phi}^{\mathrm{T}}\underset{\sim}{u}. \quad (76)$$

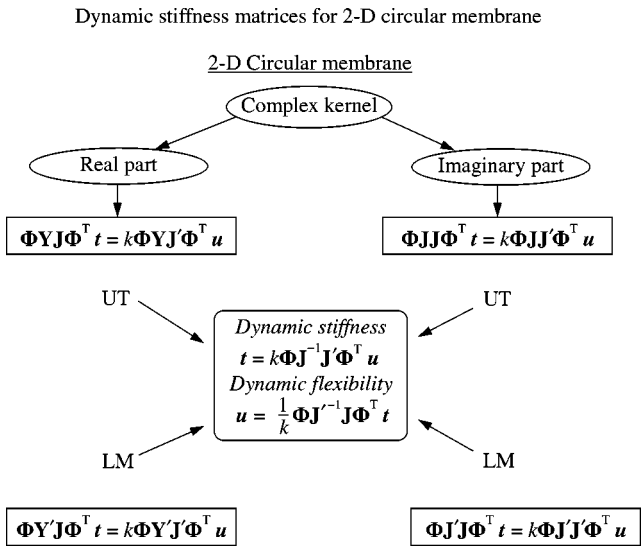


Figure 4. Dynamic stiffness and flexibility matrices for a circular membrane using the dual formulation.

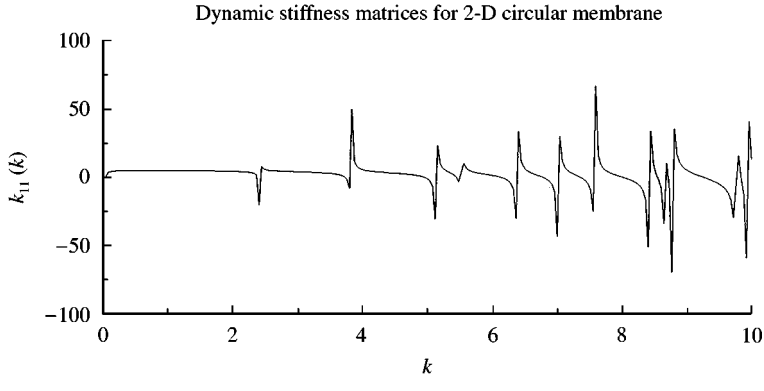


| $T_1$ | $T_2$ | $T_3$ | $T_4$ | $T_5$ | $T_6$ | $T_7$ |
|---|---|---|---|---|---|---|
| $k_1$ | $k_2$ | $k_3$ | $k_4$ | $k_5$ | $k_6$ | $k_7$ |
| 2·40 | 3·83 | 5·14 | 5·52 | 6·38 | 7·08 | 8·41 |

Figure 5. The dynamic stiffness $k_{11}$ versus $k$.

It is interesting to summarize all the results of equations (68)–(76) in Figure 4. The dynamic stiffness matrix can be expressed as

$$[K] = [U]^{-1}[T] = [L]^{-1}[M], \tag{77}$$

where $\underset{\sim}{t} = K\underset{\sim}{u}$ and $[K]$ is shown below:

$$[K] = k\mathbf{\Phi}\mathbf{J}^{-1}\mathbf{J}'\mathbf{\Phi}^{\mathrm{T}}. \tag{78}$$

The dynamic stiffness $k_{11}$ versus $k$ is shown in Figure 5. Then the dynamic flexibility matrix can be expressed as

$$[F] = [T]^{-1}[U] = [M]^{-1}[L], \tag{79}$$

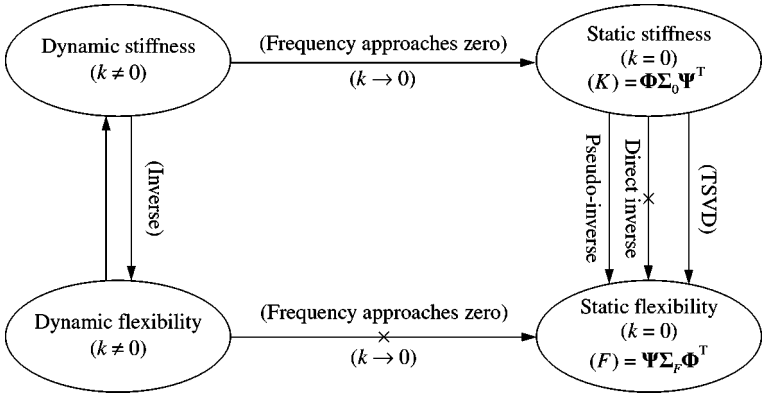


Figure 6. The derivation for the static flexibility using pseudo-inverse and TSVD.

where $\tilde{u} = F\tilde{t}$ and $[F]$ are as shown below:

$$[F] = \frac{1}{k}\,\mathbf{\Phi}\mathbf{J}'^{-1}\mathbf{J}\,\mathbf{\Phi}^{\mathrm{T}}. \tag{80}$$

The numerical results of equations (78) and (80) can be found in reference [29].

## 6. SPECIAL CASE—STATIC STIFFNESS AND STATIC FLEXIBILITY

All the above dynamic stiffness matrices have the limiting value if the value of $k$ approaches zero. This limiting matrix with elements of finite values is the static stiffness. On the contrary, the static flexibility cannot be determined directly by setting the value of $k$ to be zero in the dynamic boundary flexibility since infinite value in the elements of matrix will occur. To circumvent this problem, the truncated singular-value decomposition (TSVD) technique in conjunction with the concept of pseudo-inverse [25] is employed to calculate the static flexibility as shown in Figure 6. When $k$ approaches zero for a rod, equation (17) turns out to be

$$\begin{Bmatrix} -t(0) \\ t(1) \end{Bmatrix} = [K] \begin{Bmatrix} u(0) \\ u(1) \end{Bmatrix}, \tag{81}$$

where the static stiffness $[K]$ can be expressed as

$$[K] = \begin{bmatrix} 1 & -1 \\ -1 & 1 \end{bmatrix}. \tag{82}$$

By employing the pseudo-inverse technique, the static flexibility $[F]$ can be expressed as

$$[F] = \begin{bmatrix} \frac{1}{4} & -\frac{1}{4} \\ -\frac{1}{4} & \frac{1}{4} \end{bmatrix}. \tag{83}$$

When $k$ approaches zero for a beam, equation (66) turns out to be

$$[K] \begin{Bmatrix} \delta_1 \\ \theta_1 \\ \delta_2 \\ \theta_2 \end{Bmatrix} = \begin{Bmatrix} V_1 \\ M_1 \\ V_2 \\ M_2 \end{Bmatrix}, \tag{84}$$

where the static stiffness $[K]$ can be expressed as

$$[K] = \begin{bmatrix} 12 & 6 & -12 & 6 \\ 6 & 4 & -6 & 2 \\ -12 & -6 & 12 & -6 \\ 6 & 2 & -6 & 4 \end{bmatrix}. \tag{85}$$

By employing the pseudo-inverse technique, the static flexibility $[F]$ can be expressed as

$$[F] = \frac{1}{150} \begin{bmatrix} 2 & 1 & -2 & 1 \\ 1 & 38 & -1 & -37 \\ -2 & -1 & 2 & -1 \\ 1 & -37 & -1 & 38 \end{bmatrix}. \tag{86}$$

It is interesting to find that equations (83) and (86) match well with those derived by FEM [27, 28]. Similarly, when $k$ approaches zero, the static stiffness for circular membrane $[K]$ in equation (77) reduces to

$$[K] = \mathbf{\Phi}\, \mathbf{\Sigma}_0\, \mathbf{\Phi}^{\mathrm{T}}, \tag{87}$$

where

$$\mathbf{\Sigma}_0 = \begin{bmatrix} 0 & 0 & \cdots & \cdots & \cdots & \cdots & 0 \\ 0 & 1 & 0 & \vdots & \vdots & \vdots & \vdots \\ \vdots & 0 & 1 & 0 & \vdots & \vdots & \vdots \\ \vdots & \vdots & 0 & \ddots & 0 & \vdots & \vdots \\ \vdots & \vdots & \vdots & 0 & N-1 & 0 & \vdots \\ \vdots & \vdots & \vdots & \vdots & 0 & N-1 & 0 \\ 0 & 0 & 0 & \cdots & \cdots & 0 & N \end{bmatrix}_{2N \times 2N} \tag{88}$$

after using the asymptotic formula,

$$\lim_{k \to 0} \mathrm{J}_N(k) \approx \frac{(1/2k)^N}{\Gamma(N+1)}, \tag{89}$$

differentiation formula,

$$\mathrm{J}'_N(k) = \frac{\mathrm{J}_{N-1}(k) - \mathrm{J}_{N+1}(k)}{2} \tag{90}$$

and

$$k\mathrm{J}_N^{-1}\mathrm{J}'_N = N\left(1 - \frac{(k/2)^2}{N(N+1)}\right), \tag{91}$$

in which $\Gamma(N+1)$ is the Gamma function. By employing the pseudo-inverse technique, the static flexibility $[F]$ can be expressed as

$$[F] = K^* = \mathbf{\Phi}\, \mathbf{\Sigma}_F\, \mathbf{\Phi}^{\mathrm{T}}, \tag{92}$$

where $K^*$ denotes the pseudo-inverse of $K$ and

$$\boldsymbol{\Sigma}_F = \begin{bmatrix} 0 & 0 & \cdots & \cdots & \cdots & \cdots & 0 \\ 0 & 1 & 0 & \vdots & \vdots & \vdots & \vdots \\ \vdots & 0 & 1 & 0 & \vdots & \vdots & \vdots \\ \vdots & \vdots & 0 & \ddots & 0 & \vdots & \vdots \\ \vdots & \vdots & \vdots & 0 & \dfrac{1}{N-1} & 0 & \vdots \\ \vdots & \vdots & \vdots & \vdots & 0 & \dfrac{1}{N-1} & 0 \\ 0 & 0 & 0 & \cdots & \cdots & 0 & \dfrac{1}{N} \end{bmatrix}_{2N \times 2N}, \tag{93}$$

in which the inverse of zero diagonal term of $\boldsymbol{\Sigma}_0$ in equation (88) is set to be zero in the first diagonal element of $\boldsymbol{\Sigma}_F$ in equation (93). For demonstration, a circular membrane is considered. In this case, 10 elements ($N = 5$) are adopted in the boundary element mesh. Based on equation (87), the static stiffness can be obtained as shown below:

$$[K] = \begin{bmatrix} 15 & -7{\cdot}74 & 2{\cdot}5 & -3{\cdot}26 & 2{\cdot}5 & -3 & 2{\cdot}5 & -3{\cdot}26 & 2{\cdot}5 & -7{\cdot}74 \\ -7{\cdot}74 & 15 & -7{\cdot}74 & 2{\cdot}5 & -3{\cdot}26 & 2{\cdot}5 & -3 & 2{\cdot}5 & -3{\cdot}26 & 2{\cdot}5 \\ 2{\cdot}5 & -7{\cdot}74 & 15 & -7{\cdot}74 & 2{\cdot}5 & -3{\cdot}26 & 2{\cdot}5 & -3 & 2{\cdot}5 & -3{\cdot}26 \\ -3{\cdot}26 & 2{\cdot}5 & -7{\cdot}74 & 15 & -7{\cdot}74 & 2{\cdot}5 & -3{\cdot}26 & 2{\cdot}5 & -3 & 2{\cdot}5 \\ 2{\cdot}5 & -3{\cdot}26 & 2{\cdot}5 & -7{\cdot}74 & 15 & -7{\cdot}74 & 2{\cdot}5 & -3{\cdot}26 & 2{\cdot}5 & -3 \\ -3 & 2{\cdot}5 & -3{\cdot}26 & 2{\cdot}5 & -7{\cdot}74 & 15 & -7{\cdot}74 & 2{\cdot}5 & -3{\cdot}26 & 2{\cdot}5 \\ 2{\cdot}5 & -3 & 2{\cdot}5 & -3{\cdot}26 & 2{\cdot}5 & -7{\cdot}74 & 15 & -7{\cdot}74 & 2{\cdot}5 & -3{\cdot}26 \\ -3{\cdot}26 & 2{\cdot}5 & -3 & 2{\cdot}5 & -3{\cdot}26 & 2{\cdot}5 & -7{\cdot}74 & 15 & -7{\cdot}74 & 2{\cdot}5 \\ 2{\cdot}5 & -3{\cdot}26 & 2{\cdot}5 & -3 & 2{\cdot}5 & -3{\cdot}26 & 2{\cdot}5 & -7{\cdot}74 & 15 & -7{\cdot}74 \\ -7{\cdot}74 & 2{\cdot}5 & -3{\cdot}26 & 2{\cdot}5 & -3 & 2{\cdot}5 & -3{\cdot}26 & 2{\cdot}5 & -7{\cdot}74 & 15 \end{bmatrix}_{10 \times 10} . \tag{94}$$

The stiffness matrix $[K]$ in equation (94) is singular and symmetric as expected. According to equation (92), the static flexibility can be determined as

$$[F] = \begin{bmatrix} 2{\cdot}28 & 0{\cdot}46 & -0{\cdot}09 & -0{\cdot}57 & -0{\cdot}55 & -0{\cdot}78 & -0{\cdot}55 & -0{\cdot}57 & -0{\cdot}09 & 0{\cdot}46 \\ 0{\cdot}46 & 2{\cdot}28 & 0{\cdot}46 & -0{\cdot}09 & -0{\cdot}57 & -0{\cdot}55 & -0{\cdot}78 & -0{\cdot}55 & -0{\cdot}57 & -0{\cdot}09 \\ -0{\cdot}09 & 0{\cdot}46 & 2{\cdot}28 & 0{\cdot}46 & -0{\cdot}09 & -0{\cdot}57 & -0{\cdot}55 & -0{\cdot}78 & -0{\cdot}55 & -0{\cdot}57 \\ -0{\cdot}57 & -0{\cdot}09 & 0{\cdot}46 & 2{\cdot}28 & 0{\cdot}46 & -0{\cdot}09 & -0{\cdot}57 & -0{\cdot}55 & -0{\cdot}78 & -0{\cdot}55 \\ -0{\cdot}55 & -0{\cdot}57 & -0{\cdot}09 & 0{\cdot}46 & 2{\cdot}28 & 0{\cdot}46 & -0{\cdot}09 & -0{\cdot}57 & -0{\cdot}55 & -0{\cdot}78 \\ -0{\cdot}78 & -0{\cdot}55 & -0{\cdot}57 & -0{\cdot}09 & 0{\cdot}46 & 2{\cdot}28 & 0{\cdot}46 & -0{\cdot}09 & -0{\cdot}57 & -0{\cdot}55 \\ -0{\cdot}55 & -0{\cdot}78 & -0{\cdot}55 & -0{\cdot}57 & -0{\cdot}09 & 0{\cdot}46 & 2{\cdot}28 & 0{\cdot}46 & -0{\cdot}09 & -0{\cdot}57 \\ -0{\cdot}57 & -0{\cdot}55 & -0{\cdot}78 & -0{\cdot}55 & -0{\cdot}57 & -0{\cdot}09 & 0{\cdot}46 & 2{\cdot}28 & 0{\cdot}46 & -0{\cdot}09 \\ -0{\cdot}09 & -0{\cdot}57 & -0{\cdot}55 & -0{\cdot}78 & -0{\cdot}55 & -0{\cdot}57 & -0{\cdot}09 & 0{\cdot}46 & 2{\cdot}28 & 0{\cdot}46 \\ 0{\cdot}46 & -0{\cdot}09 & -0{\cdot}57 & -0{\cdot}55 & -0{\cdot}78 & -0{\cdot}55 & -0{\cdot}57 & -0{\cdot}09 & 0{\cdot}46 & 2{\cdot}28 \end{bmatrix}_{10 \times 10} . \tag{95}$$

Equation (95) can be seen as an analytical solution for the static flexibility in a discrete system.

## 7. CONCLUSIONS

In this paper, two approaches, using the real-part and imaginary-part kernels, were developed to construct the same dynamic stiffness and flexibility matrices. Three examples, rod, beam and circular membrane, were demonstrated to show the validity of the present formulations. It is also found that similar mathematical structures can be found for the influence matrices in dual BEM. True and spurious eigensolutions can be determined easily and separated efficiently at the stage of determining the stiffness matrix. Instead of using the complex-valued formulation, the proposed method for determining the stiffness or flexibility is time saving from the computational point of view since only the real or imaginary part is considered. Also, the static flexibility can be derived and solved by using the pseudo-inverse technique.

## ACKNOWLEDGMENTS

Financial support from the National Science Council under Grant No. NSC-89-2211-E-019-021 for National Taiwan Ocean University is gratefully acknowledged.

## REFERENCES

1. R. C. HIBBELER 1997 *Structural Analysis*. New York: Prentice-Hall.
2. R. W. CLOUGH and J. PENZIEN 1975 *Dynamics of Structures*. New York: McGraw-Hill.
3. P. MARIO and D. LAM 1975 *International Journal for Numerical Methods in Engineering* **9**, 449–459. Power series expansion of the general stiffness matrix for beam elements.
4. P. MARIO 1973 *Computers and Structures* **3**, 385–396. Mathematical observations in structural dynamics.
5. C. M. CHANG 1998 *Master thesis*, *Department of Harbor and River Engineering*, *National Taiwan Ocean University*, *Taiwan*. Analysis of natural frequencies and natural modes for rod and beam problems using multiple reciprocity method (MRM).
6. W. YEIH, J. T. CHEN and C. M. CHANG 1999 *Engineering Analysis with Boundary Elements* **23**, 339–360. Applications of dual MRM for determining the natural frequencies and natural modes of an Euler–Bernoulli beam using the singular value decomposition method.
7. J. R. BANERJEE 1996 *Journal of Sound and Vibration* **194**, 573–585. Exact dynamic stiffness matrix for composite Timoshenko beams with applications.
8. J. R. BANERJEE 1998 *Computers and Structures* **69**, 197–208. Free vibration of axially loaded composite Timoshenko beams using the dynamic stiffness matrix method.
9. J. E. LUCO and R. A. WESTMANN 1972 *Journal of Applied Mechanics* **39**, 527–534. Dynamic response of a rigid footing bounded to an elastic half space.
10. J. LYSMER and R. L. KUHLEMEYER 1969 *Journal of Engineering Mechanics* **95**, 859–877. Finite dynamic model for infinite media.
11. J. P. WOLF and C. SONG 1994 *Earthquake Engineering and Structural Dynamics* **23,** 1181–1198. Dynamic-stiffness matrix in time domain of unbounded medium by infinitesimal finite element.
12. J. X. ZHAO, A. J. CARR and P. J. MOSS 1997 *Earthquake Engineering and Structural Dynamics* **26**, 115–133. Calculating the dynamic stiffness matrix of 2-D foundations by discrete wave number indirect boundary element methods.
13. J. L. WEARING and O. BETTAHAR 1996 *Engineering Analysis with Boundary Elements* **16,** 261–271. The analysis of plate bending problems using the regular direct boundary element method.
14. A. Y. T. LEUNG 1993 *Dynamic Stiffness and Substructures*. London: Springer-Verlag.
15. J. T. CHEN, C. X. HUANG and K. H. CHEN 1999 *Computational Mechanics* **24**, 41–51. Determination of spurious eigenvalues and multiplicities of true eigenvalues using the real-part dual BEM.

16. J. T. CHEN, S. R. KUO and C. X. HUANG 1999 *IUTAM/IACM/IABEM Symposium on BEM*, *Cracow*, *Poland*, 18–19. Analytical study and numerical experiments for true and spurious eigensolutions of a circular cavity using the real-part dual BEM.
17. J. R. CHANG, W. YEIH and J. T. CHEN 1999 *Computational Mechanics* **24,** 29–40. Determination of natural frequencies and natural modes using the dual BEM in conjunction with the domain partition technique.
18. J. T. CHEN, C. X. HUANG and F. C. WONG 2000 *Journal of Sound and Vibration* **230**, 230–219. Determination of spurious eigenvalues and multiplicities of true eigenvalues in the dual multiple reciprocity method using the singular value decomposition technique.
19. J. T. CHEN and F. C. WONG 1998 *Journal of Sound and Vibration* **217**, 75–95. Dual formulation of multiple reciprocity method for the acoustic mode of a cavity with a thin partition.
20. D. Y. LIOU, J. T. CHEN and K. H. CHEN 1999 *Journal of the Chinese Institute of Civil and Hydraulic Engineering* **11,** 299–310 (in Chinese). A new method for determining the acoustic modes of a two-dimensional sound field.
21. W. YEIH, J. R. CHANG, C. M. CHANG and J. T. CHEN 1999 *Advances in Engineering Software* **30**, 459–468. Applications of dual MRM for determining the natural frequencies and natural modes of a rod using the singular value decomposition method.
22. Y. C. WU 1999 *Master thesis*, *National Taiwan Ocean University*, *Taiwan*. Applications of the generalized singular value decomposition method to the eigenproblem of the Helmholtz equation.
23. I. L. CHEN, J. T. CHEN, S. R. KUO and M. T. LIANG 2001 *Journal of Acoustical Society of America* **109**, 982–999. A new method for true and spurious eigensolutions of arbitrary cavities using the CHEEF method.
24. T. F. CHEN and P. C. HANSEN 1990 *SIAM*, *Journal Science Statistics Computation* **11**, 519–530. Computing truncated singular value decomposition least squares solutions by rank revealing QR-factorizations.
25. O. CHRISTENSEN 1995 *Journal of Mathematical Analysis and Applications* **195**, 401–414. Frames and pseudo-inverse.
26. M. W. BERRY, Z. DRAMAC and E. R. JESSUP 1999 *SIAM Review* **41**, 335–362. Matrices, vector spaces and information retrieval.
27. C. A. FELIPPA and K. C. PARK 1997 *Computer Methods Applied Mechanics Engineering* **149**, 319–337. A direct flexibility method.
28. C. A. FELIPPA, K. C. PARK and M. R. JUSTINO FILHO 1998 *Computers and Structures* **68**, 411–418. The construction of free–free flexibility matrices as generalized stiffness inverses.
29. J. T. CHEN, I. L. CHUNG and I. L. CHEN 2001 *Computational Mechanics* **27**, 75–87. Analytical study and numerical experiments for true and spurious eigensolutions of a circular cavity using an efficient mixed-part dual BEM.